

Progress in HTS Trapped Field Magnets: J_c , Area, and Applications

Roy Weinstein, Yanru Ren, Jianxiong Liu, Ravi Sawh, Drew Parks, Charles Foster*, Victor Obot**, G. Dickey Arndt***, and Alan Crapo****

Institute for Beam Particle Dynamics and Texas Center for Superconductivity,
University of Houston, Houston, TX 77204-5506

*Indiana University Cyclotron Facility, Bloomington, IN 47405

**Dept. of Mathematics, Texas Southern University, Houston, TX 77004

***Johnson Space Center, NASA, Houston, TX 77058

****Emerson Electric Co., St. Louis, MO 63136

Abstract

Progress in trapped field magnets is reported. Single YBCO grains with diameters of 2 cm are made in production quantities, while 3 cm, 4 1/2 cm and 6 cm diameters are being explored. For single grain tiles: $J_c \sim 10,000 \text{ A/cm}^2$ for melt textured grains; $J_c \sim 40,000 \text{ A/cm}^2$ for light ion irradiation; and $J_c \sim 85,000 \text{ A/cm}^2$ for heavy ion irradiation. Using 2 cm diameter tiles bombarded by light ions, we have fabricated a mini-magnet which trapped 2.25 Tesla at 77K, and 5.3 Tesla at 65K. A previous generation of tiles, 1 cm x 1 cm, was used to trap 7.0 Tesla at 55K. Unirradiated 2.0 cm tiles were used to provide 8 magnets for an axial gap generator, in a collaborative experiment with Emerson Electric Co. This generator delivered 100 Watts to a resistive load, at 2265 rpm. In this experiment activation of the TFMs was accomplished by a current pulse of 15 ms duration. Tiles have also been studied for application as a bumper-tether system for the soft docking of spacecraft. A method for optimizing tether forces, and mechanisms of energy dissipation are discussed. A bus bar was constructed by welding three crystals while melt-texturing, such that their a,b planes were parallel and interleaved. The bus bar, of area $\sim 2 \text{ cm}^2$, carried a transport current of 1000 amps, the limit of the testing equipment available.

I. Introduction

Our research group has worked to develop trapped field magnets (TFM), made of high temperature superconductor (HTS), since about January of 1988. We will report here progress on TFM since the Third World Congress on Superconductivity in Munich Germany, in 1993 (WCS III)⁽¹⁾. We will also report progress on certain applications since WCS III. Progress prior to that date is reported in Ref. 1, and in citations therein.

Models of the persistent current flow within a TFM⁽²⁻⁵⁾ show that the maximum trappable field, $B_{t,max}$, is given approximately by

$$B_{t,max} \propto J_c f(d) \quad \text{Eq. 1}$$

where J_c is the critical current, d is the diameter of the contiguous current carrying region (a so-called grain, or tile), and $f(d)$ is a complicated monotonically increasing function of d . For example in the present range of interest (but not in general), $f(d) \sim d^{1/2}$. A number of analyses of trapped field magnets in the literature assume incorrect variations of Eq. 1. These lead to disagreements with data, which are then erroneously attributed to TFM properties.

Guided by Eq. 1 our major efforts are directed to: (a) increase J_c ; (b) increase d . In addition, we study basic properties of pinning centers to reduce creep. Our studies of creep will be reported elsewhere.

II. Improvements in Grain Diameter

At WCS III we reported a grain diameter of just over 2 cm. This had been achieved in exploratory experiments, not in regular production. In fact, the yield of usable TFMs, per processed ingot of $YBa_2Cu_3O_7$ (Y123), was only circa 15%.

At present two cm grains of Y123 are regularly produced. The yield of usable TFMs of 2 cm size, per processed unit of Y123, is now about 95%. In addition, tiles of 3.0, 4.5 and 6.2 cm have been produced on an exploratory basis. Also, using the same techniques, we produce 6 cm x 2 cm x 2 cm bus bars. These will be discussed in Sec. VI.

The tiles, or grains, reported at WCS III were produced by the melt-texture (MT) process.⁽⁶⁾ The larger tiles now produced reliably were achieved by (a) optimization of the MT temperature profile (b) addition of circa 1% Pt, to control the shape of Y_2BaCuO_5 (Y211) inclusions in the Y123 tile, (c) the use of $SmBa_2Cu_3O_7$ (SM123) seeds, to initiate predominantly single grain structure, and (d) the use of Y211 platforms, on which the Y123 rests, which absorb excess Cu-Ba liquid formed during the process.

The single grain structure of the melt-textured tiles can be determined by measuring the trapped magnetic field, e.g., across the face of the tile, and comparing to theory.^(4,5) An example of this is shown in Fig. 1. For this type of analysis an automated field scanning device is used.⁽⁴⁾

At the time of WCS III, the trapped field routinely achieved in a single tile, prior to irradiation, was ~1,500 Gauss⁽¹⁾, and was ~5,000 Gauss after irradiation. (The exploratory tile with $d \sim 2$ cm trapped 2,200 G prior to irradiation.) At present, routine 2cm tiles trap 4300-4500 G prior to irradiation, and over 12,000 G after irradiation.

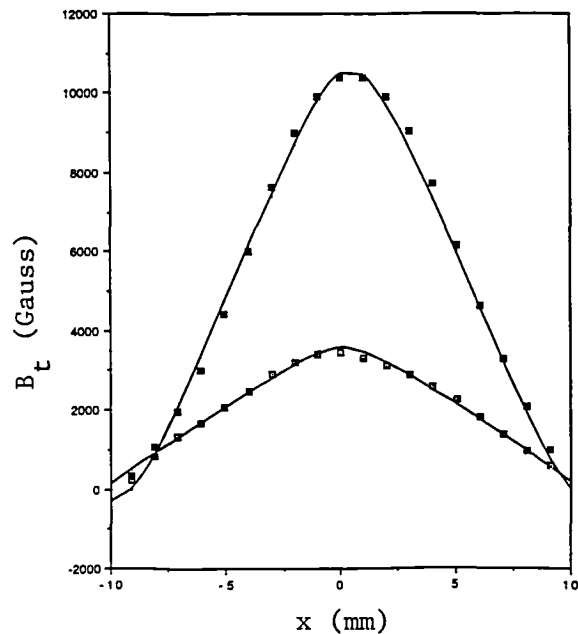


Fig. 1. Trapped field vs. position along the diameter of a single 2 cm grain of Y123. Lower points are before, and upper points are after p^+ bombardment. Solid curves are the theory of Refs. 4,5.

III. Improvement in J_c

J_c is determined in part by the quality of the melt-textured grain, especially by the absence of weak links. For a good MT grain of Y123, $J_c = 8\text{-}10,000 \text{ A/cm}^2$.

J_c is also dependent upon the presence of pinning centers, which are small diameter regions of poor superconductivity within the tile. We have used Y211, finely divided, to introduce chemical pinning centers, and increase J_c ⁽¹⁾. This showed some success and increased J_c to $10\text{-}13,000 \text{ A/cm}^2$. We have also used bombardment by light ions (protons and He) to damage the Y123 crystals and increase J_c ⁽⁷⁾. This increases J_c markedly, to $\sim 40,000 \text{ A/cm}^2$.

We are presently pursuing a technique^(7,8) which permits production of columnar pinning centers in MT Y123. There is strong evidence⁽⁹⁾ that columnar pinning centers (a) result in higher J_c , particularly at higher temperatures (e.g. 77K); and (b) increase the irreversibility line, thus allowing the production, ultimately, of higher B_{trap} . Increases of J_c by a factor of 3, and irreversibility fields by a factor of 2 have been reported at 77K.⁽⁹⁾

Most methods used to produce columnar pinning centers are unable to produce large scale devices. For example, Ref. 9 utilized 580 MeV Sn ions to cause such defects. However, such ions have a range of only $20 \mu\text{m}$ in Y123.

In order to produce columnar defects in larger scale devices we have developed a method in which the Y123 is seeded with U^{235} and then irradiated with thermal neutrons, n^0_t . The n^0_t induce fission in the U^{235}



The total energy of the fission fragments is circa 200 MeV, and their range is $\sim 20 \mu\text{m}$. The average $Z_f \sim 46$, close to the value for tin, for which $Z = 50$.

The U^{235} seeding can be made uniform over large volumes, and the n^0_t penetrates to large distances. Thus a uniform volume distribution of columnar centers can be achieved.

The U^{235} must be dispersed in MT Y123 such that the spacing between U^{235} globules is $< 20 \mu\text{m}$. Also, the U^{235} globules themselves must be $\ll 6 \mu\text{m}$ in diameter, so that they do not self absorb the fission fragments. Fig. 2 shows the U distribution actually achieved. Fig. 3 shows results of the first test of this U^{235}/n method. In this experiment $J_c = 85,000 \text{ A/cm}^2$ was achieved. This is twice the J_c achieved by our proton or helium bombardments.^(1,7)

The U/n method is inhibited by the effect that U addition has on the formation of good quality melt-textured Y123 grains. Addition of U beyond about 0.5% by weight degrades the melt texturing.^(7,8) In our initial experiments, depleted U was used, in which only 0.4% of U^{235} remained. The amount of U needed, in order to provide

sufficient U^{235} , prevented us from exploring the maximum J_c achievable by this method. At present we are experimenting instead with 95% enriched U^{235} . Using enriched U^{235} in place of the depleted U, reduces the mass of U needed, at a given fluence, by a factor of over 200. Present experiments seek an optimum for fluence x mass of U^{235} , in order to maximize J_c .

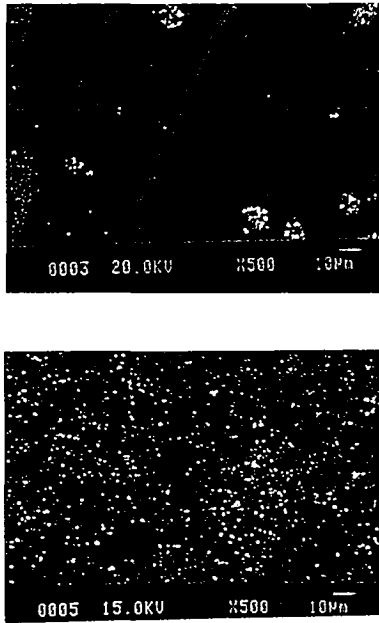


Fig. 2. Top: SEM micrograph of MT Y123 plus 0.6% depleted uranium. Bottom: Same as top after careful U dispersion.

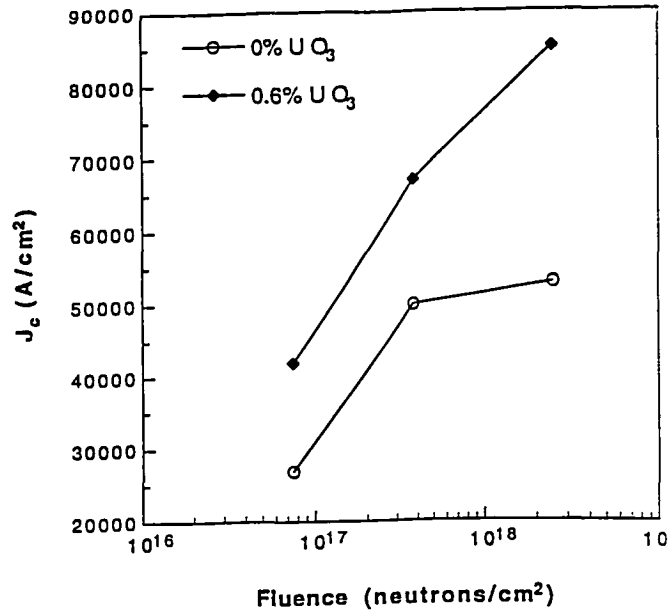


Fig. 3. Top: Effect of n°_t bombardment of Y123 plus 0.6% depleted uranium. Bottom: control sample.

IV. Temperature Dependence

At the time of WCS III, we had strong evidence of a rapid increase in $B_{t,max}$ as T was decreased.^(10,11) Such an increase is expected from Eq. 1 and the fact that J_c generally increases as T decreases. A study of J_c vs. T for unirradiated melt-textured Y123 was done on small samples,⁽¹²⁾ utilizing a vibrating sample magnetometer (VSM). Generally VSMs have small activation regions, and cannot analyze samples larger than a few millimeters. For $T < 65$, the result of our tests was an excellent fit to the equation

$$J_c(T) = J_c(65K) \times (T_c - T / T_c - 65)^2 \quad \text{Eq. 3}$$

Fig. 4 shows these results. A sample produced by Murakami, at ISTE⁽¹³⁾ by the MPMG method is shown for comparison. It exhibits the same $J_c(T)$ dependence, albeit with J_c about a factor of 2 lower. From Eq. 3 and Eq. 1 we conclude that B_t should have

the same temperature dependence as given in Eq. 3, at least for unirradiated Y123. We will consider irradiated Y123 next.

V. Mini-Magnets

We fabricate mini-magnets from a collection of single tiles. Two such magnets were each fabricated from 6 irradiated tiles, $\sim 1.2 \text{ cm} \times 1.2 \text{ cm} \times 0.3 \text{ cm}$. In order to test whether Eq. 3 applies to irradiated tiles as well as non-irradiated tiles, these mini-magnets were tested at various temperatures.⁽⁸⁾ Fig. 5 shows the results. The solid curve, which fits the data reasonably well, is calculated from Eq. 3. Thus, at least for $T \geq 55\text{K}$, Eq. 3 also applies to fabrications made from tiles irradiated by light ions.

Note in Fig. 5 that the trapped field observed is circa 1.5 Tesla at 77K⁽¹¹⁾, 4.0T at 65K⁽⁸⁾ and 7.0T at 55K⁽⁸⁾. The latter two measurements were record trapped fields, eclipsing the record of 2.3T at 4K, set at Stanford in 1977⁽¹⁵⁾. Fig. 6 shows the activation curve taken at 55K, in which 7T is trapped. Fig. 7 shows more recent results on a mini-magnet made of 2 cm diameter tiles irradiated by protons. Here 2.3 T is achieved at 77K, and 5.3 T at 65K. We expect this generation of tiles to exceed $B_{t,\text{max}} = 10\text{T}$ at 55K in tests which are in progress.

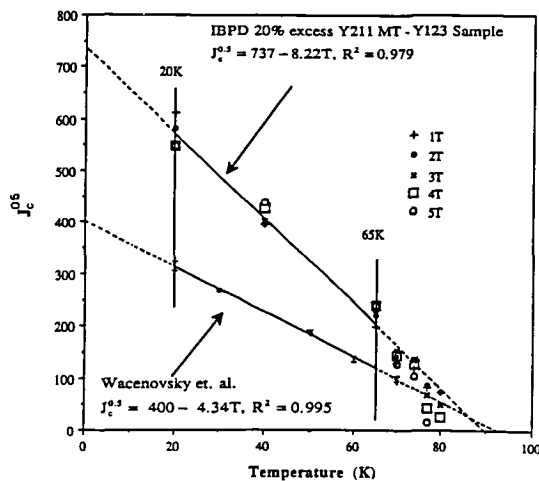


Fig. 4. $J_c^{1/2}$ vs. T , at various fields, measured by VSM on non-irradiated Y123. Top line: IBPD/TCSUH sample. Lower line is ISTEC sample of Ref. 13.

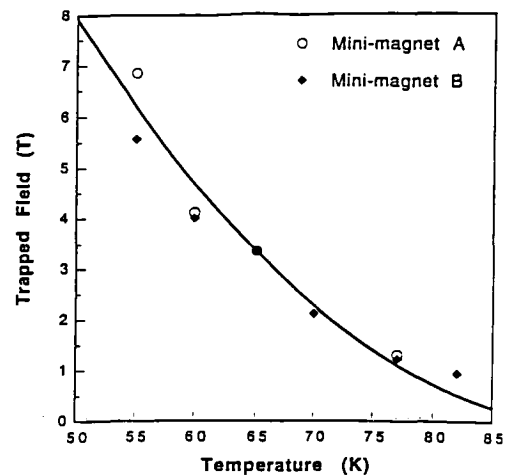


Fig. 5. B_{trap} vs. T for 2 mini-magnets, normalized at 65K. Solid line is from fit of Fig. 4.

VI. Bus Bar

We developed a technique to weld-while-texturing which allows a number of tiles to be welded into a single grain. Using this, we welded 3 tiles together, each $2 \times 2 \times 1 \text{ cm}^3$. From the trapped field we estimate that this bus bar, 6 cm long, will carry a transport

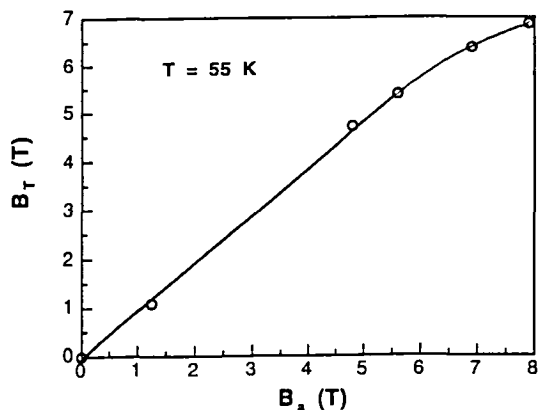


Fig. 6. B_T vs. applied field, B_a , at 55K for 6-tile mini-magnet. At each point the Y123 is field cooled at the value of B_a shown. Tiles have area $\sim 1 \text{ cm}^2$.

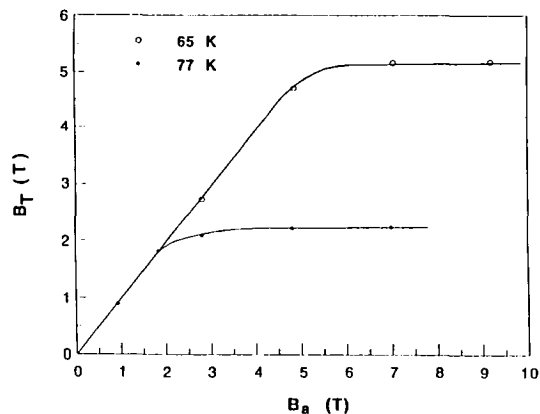


Fig. 7. B_T vs. B_a for 2-tile mini-magnet. Data as in Fig. 6. Tiles have area $\sim 3.1 \text{ cm}^2$

current of 2000 A at 77K. In order to experimentally test the transport current in the bus bar, silver leads were epoxied to the Y123, using silver epoxy. The transport current for this device was tested in the laboratory of Kamel Salama⁽¹⁵⁾. The bar successfully carried 1000A of transport current, which is the maximum for which the lab can test.

In principal this technique will work for bus bars of length up to 40 cm, made with our present equipment.

VII. Generator

Fig. 8 is a schematic of a generator run in collaboration with Emerson Electric Co.⁽¹⁶⁾ The rotor has 8 iron posts on which 8 TFMs were mounted, each 2 cm diameter. The stator of the generator is composed of copper wire, run at 77K. The copper is wound in an 8-pole, 3-phase configuration. The rotor was motor driven, and the generator output went to a three-phase variable resistive load.

In two separate runs the TFMs were (a) field cooled, and (b) zero field cooled. In the first case the TFMs were cooled in an applied field provided by constant current through the stator wires. Current, and therefore fields, were limited by the desire to avoid burning the stator insulation. The TFMs did not limit the field. Activating fields of ≤ 2500 Gauss, limited by armature heating, resulted in TFM fields of ~ 1800 G. In the second case the TFMs were cooled at zero field, and then a 15 ms *pulse* of current was put through the stator. This produced an activating field of ~ 5000 G, which resulted in a trapped field of ~ 2600 G. This is still less than the 3500-4000 G those particular TFMs could trap. Higher ZFC fields can be obtained with higher pulsed voltage (until inter-wire arcing occurs on the stator).

The generator was run at a large variety of speeds up to 2265 rpm, and supplied up to 100 Watts⁽¹⁶⁾ to the load.

We had previously used the configuration of Fig. 8 as a motor.^(1,17) The motor, run with an earlier generation of tiles ~ 1 cm x 1 cm x 0.3 cm, achieved an output of 19 Watts.⁽¹⁷⁾

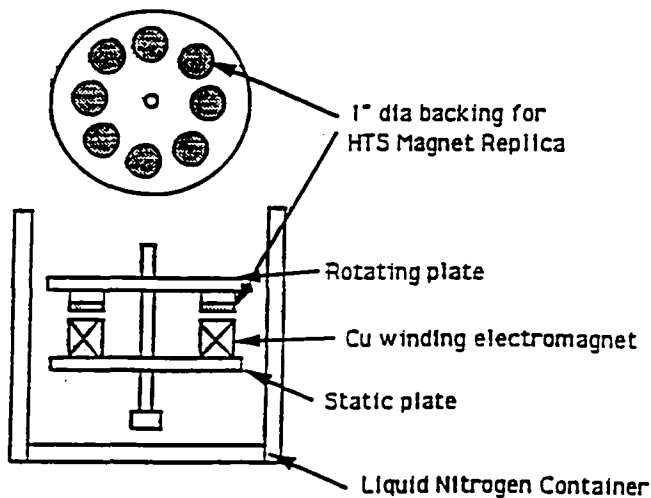


Fig. 8. Schematic of Emerson Electric/TCSUH motor. Top: view of rotor, with 1" diam. iron rods. Bottom: Side view of rotor, stator and cryostat.

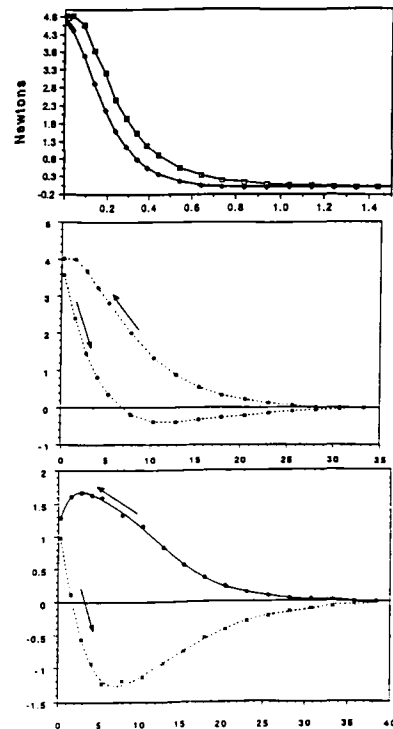


Fig. 9. Force (N) vs. distance (mm) for $B_a/B_{t,max} = 0.67$ (top); 1.39 (middle); 2.74 bottom.

VIII. Bumper/Tether

Assume a TFM is cooled in zero field and therefore has no trapped field. Assume that a ferromagnet is then brought close to the TFM. As the magnet approaches, the superconductor first acts like a mirror image of the approaching ferromagnet, and repels it. If the approaching ferromagnet has momentum it will continue to approach the superconductor until it is stopped by the repelling force. It then continues to be repelled, and accelerates in the reverse direction. Sig Fig. 9.

The nature of the current is possibly best understood by the Bean model.⁽²⁾ After such a collision, as the magnet and TFM separate, an attractive force develops at some

distance. This cycle is shown in Fig. 9. The detailed behavior of the repulsion/attraction depends upon the ratio of the ferromagnet field, B_{Fe} , to $B_{t,max}$ of the TFM. Fig. 9 shows three cases, with varying $B_{Fe}/B_{t,max}$. The largest tethering force occurs for $B_{Fe}/B_{t,max} > 2$, after which $F_{Tether}/F_{Bumper} \sim \text{constant}$.

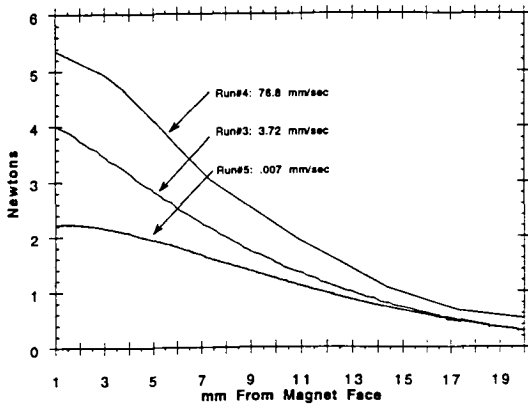


Fig. 10. Velocity dependence of bumper/tether force over 4 orders of magnitude in v .

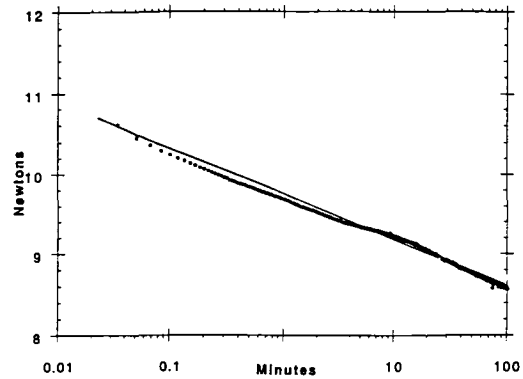


Fig. 11. Decay (creep) of force (circles) following rapid approach.

Because of the force pattern shown in Fig. 9, an array of TFMs can act first as a collision softener and then as a tether. If two spacecraft are approaching, and one has a ferro or electromagnet at the bow, while the other has an array of Y123 TFMs, forces of several tons are achievable for arrays of modest size. We believe that such an array can be a valuable backup to an aerospace docking system.

We have explored such a system to learn its characteristics. One such characteristic is that the repulsive force is velocity dependent. This effect is shown in Fig. 10. The basic source of this velocity dependence is creep. Fig. 11 shows the creep, as it effects the force, following a “sudden” collision (which took place in tenths of a second). The repelling force, as a function of time, is essentially a straight line when plotted vs. $\log t$ as is expected for creep. For low velocities, the creep reduces F_{Bumper} in the time it takes for the separation to decrease. The force is thus larger for higher relative velocities, which is desirable.

By studying the energy stored in the magnetic field of the TFM after the collision, and the energy losses to creep, we have thus far accounted for about 85% of the energy of the collision. The time dependence of the conversion of some of this energy to heat is used to place constraints on the cooling system for the TFM in the bumper/tether system.

This test also provides an alternate method to study creep at relatively short times. When creep is studied by using an electromagnet to activate a TFM, it is difficult to study creep at times $t < 1$ min. The collision study described above permits observation of creep to ~ 0.1 second. Pulsed coils are needed to probe still shorter times. Creep can, of course, also be studied by, e.g., the method of VSM.

This work is supported in part by grants from the Texas, through the Texas Center for Superconductivity at the University of Houston and the Texas Advanced Technology Program, and by grants from NASA, and the Electric Power Research Institute.

References

1. R. Weinstein, Invited Paper, Proc. World Congress on Superconductivity III, Munich, pg. 1145, Pergamon Press (1992)
2. C.P. Bean, Phys. Rev. Lett., 8, 250 (1962); Rev. Mod. Phys., 36, 31 (1964)
3. Y.B. Kim, C.F. Hempstead, A.R. Strand, Phys. Rev., 129, 528 (1963)
4. I.G. Chen, J. Liu, R. Weinstein, K. Lau, Jour. Appl. Phys., 72, 1013 (1992)
5. J. Liu, I.G. Chen, R. Weinstein, J. Xu, Jour. Appl. Phys., 73, 6530 (1993)
6. V. Selvamanickam, L. Gao, K. Sun, K. Salama, Appl. Phys. Lett., 54, 2352 (1989)
7. R. Weinstein, et al, Invited Paper, Proc. International Workshop on Superconductivity, Kyoto, Japan (June 1994)
8. R. Weinstein, Y. Ren, J. Liu, I.G. Chen, R. Sawh, C. Foster, and V. Obot, Proc. Int. Sympo. on Superconductivity, Hiroshima, Springer Verlag, in press (1993)
9. L. Civale, A.D. Marwick, T.K. Worthington, M.A. Kirk, J.R. Thompson, L. Krusin-Elbaum, Y. Sun, J.R. Clem, F. Holtzberg, Phys. Rev. Lett., 67, 648 (1991)
10. R. Weinstein, I.G. Chen, J. Liu, and K. Lau, Jour. Appl. Phys. 70, 6501 (1991)
11. R. Weinstein, I.G. Chen, J. Liu, and J. Xu, Jour. Appl. Phys., 73, 6533 (1993)
12. I.G. Chen, J. Liu, Y. Ren, R. Weinstein, G. Kozlowski, and C. Oberly, Appl. Phys. Lett., 62, 3366 (1993)
13. M. Wacenovskiy, R. Miletich, H. Weber and M. Murakami, Supercond. Sci. Technol. 5, S184 (1992)
14. M. Rabinowitz, H. Arrowsmith, S. Dahlgren, Appl. Phys. Lett., 30, (11), 607 (1977)
15. K. Salama, ME Dept., and TCSUH, Univ of Houston, Houston, TX 77204
16. R. Weinstein, A. Crapo and R.P. Sawh, contributed paper to Applied Supercond. Conf., Boston (Oct 1994)
17. C. Gillespie, Editor, Superconductor Industry, Pg. 31, Spring Issue (1993)